Zeszyty Energetyczne, Tom VII
Wyzwania naukowe w dobie światowej transformacji energetycznej
2020, s. 403–414

Computational Fluid Dynamics Simulation of Gas–Liquid Multiphase Flow in T-junction for CO_2 Separation

Sylwia Wrzesień[1], Paweł Madejski[1], Paweł Ziółkowski[2]

[1]AGH University of Science and Technology,
Department of Power Systems and Environmental Protection Facilities

[2]Gdansk University of Technology,
Department of Energy and Industrial Apparatus

e-mail: wrzesien@student.agh.edu.pl

Abstract

The article presents the results of a computational fluid dynamics (CFD) analysis of gas-liquid multiphase flow. The simulation was conducted using CFD code and the Euler–Euler approach. The presented study relates to the non–reactive, steady-state, turbulent flow of water and carbon dioxide mixture in a 3D pipe. Separation phenomenon between phases is observed. The solution was obtained using a mixture model. Different values of carbon dioxide volume fraction were taken into account in the analysis of the results. The analysed cases were compared thanks to the obtained calculations results. The main purpose of the simulations was to show streamlines, velocity, pressure, and volume fraction distribution that could be useful in developing pipeline systems in many industrial applications, especially for CO_2 separators.

Keywords: CFD, Computational Fluid Dynamics, Multiphase Flow, Numerical Simulations, T-junction

1. Introduction

In this study, numerical simulations of gas–liquid multiphase flow are presented. Flow analysis was performed with the use of computational fluid dynamics (CFD) and the Euler–Euler approach. The water–carbon dioxide mixture is flowing upwards in a 3D pipe and then splitting near the horizontal arm. The purpose of the calculations was to obtain streamlines, velocity, pressure, and volume fraction distributions that could be useful in observing the multiphase flow phenomena occurring in pipeline systems. In practical terms, phase separation is used in separators, including those for CO_2 capture [1]. The Euler–Euler approach to multiphase flow modelling was used. The solution was obtained using a mixture model. After completing the calculations, the results were analysed by taking into consideration different values of carbon dioxide volume fraction.

T-junctions are found in a large number of pipeline systems, mainly used to direct the flow from the main branch into several ducts, which leads to the stream being split. They may vary in the number of ducts and shapes. On the other hand, the situation can also be considered as the reverse, where a few flow streams converge into a single pipe. Although many studies in this area have already been done, the aim was to understand the nature of gas–liquid multiphase flows in T-junctions, which is of critical engineering and scientific importance [2]–[6]. Another aspect is further curving the shape to introduce centrifugal force and separate the two phases more efficiently.

The main purpose of the work is to determine the pressure velocity field and the proportions of individual phases in the T-junction using the ANSYS Fluent code [7]. The model presented herein can be used as the basis for analysing CO_2 separators in zero-emission and negative emission gas power plants.

2. Categorization of Different Flowe Regimes

Gas–liquid flows in ducts and separators may exhibit many different forms. These flow regimes can be sub-divided into three specific categories: dispersed flows, mixed or transitional flows, and separated flows [8]. The most common examples are dispersed flows, which consider the motion of bubbles in a liquid flow and the motion of liquid droplets in a gas. These two examples are distinguished by considering which phase is taken as the continuous phase and which phase is taken as the dispersed phase. For the first example, the liquid is taken as the continuous phase and the bubbles are considered discrete constituents of the dispersed phase. For the second example, the gas is taken as the continuous phase and the droplets are now considered finite fluid particles of the dispersed phase. These bubbles or

droplets are permitted to change shape freely within the continuous phase, taking various forms that combine dispersed and separated flow regimes, observed through many experiments [5], [6].

In addition to dispersed flows, gas–liquid flows may also assume other complex interfacial structures, namely separated flows and mixed or transitional flows. The transitional or mixed flows represent the transition state between the dispersed flows and separated flows. Due to many phase change processes – mainly coalescence and break-up – there are bubble–bubble interactions, which lead to a change of interfacial structures. At higher gas flow rates, the flow may transit to the annular flow regime, forming a liquid film on the pipe wall. These two examples can be categorized as separated flows. Figure 1 summarises the various configurations that can be found for gas–liquid flows [9].

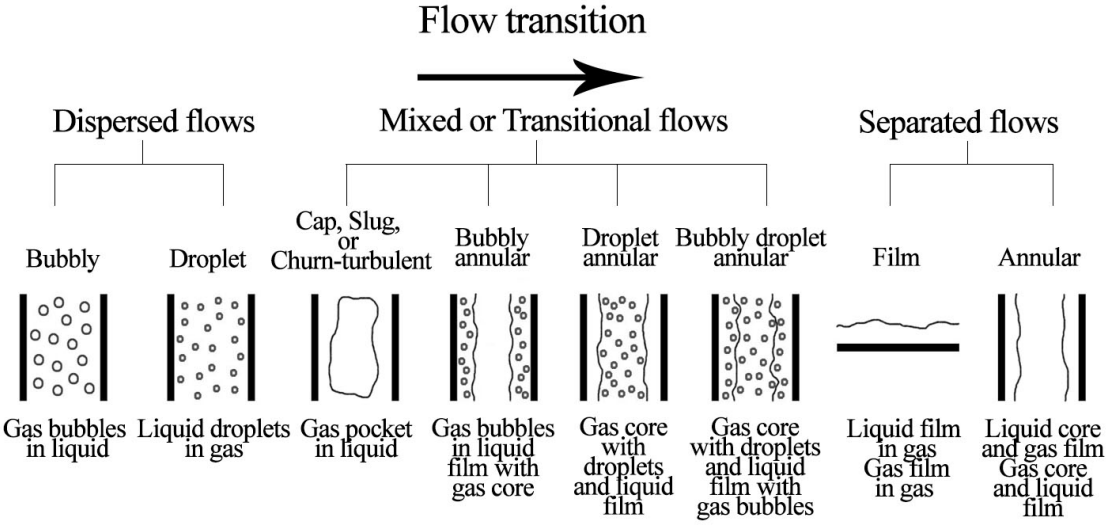

Fig. 1. Classification of gas–liquid flows (made for [8])

3. Governing Equations for Multiphase Flows

From a mathematical point of view, multiphase flow problems are notoriously difficult and much of what is known has been obtained by experimentation and scaling analysis [2]. The gas bubbles can be considered finite fluid particles of the disperse phase co-flowing, with the continuum liquid being the carrier phase [9].

3.1. Equations of Motion for Continuous Phase

The basic equations of fluid motion for each continuous phase can be obtained by first identifying the appropriate fundamental principles from the conservation laws in physics, which are conservation of mass (Eq. (1)), Newton's second law for the conservation of momentum (Eq. (2)) and the first

law of thermodynamics for the conservation of energy (Eq. (3)). These physical principles are later applied to a suitable model of the fluid flow and the mathematical equations that embody such physical principles are eventually extracted from the model under consideration. Effective conservation equations of mass for the continuous phase are defined as in Equation (1) [8]:

$$\frac{\partial}{\partial t}\left(\alpha^k \rho^k\right) + \mathrm{div}\left(\alpha^k \rho^k \mathbf{v}^k\right) = \Gamma'^k \tag{1}$$

where t is the time and $\frac{\partial}{\partial t}$ refers to the local time derivative, a^k is the volume fraction, ρ^k represents the density of each component, $\mathbf{v}^k$ is velocity of each component, Γ'^k is the interfacial mass transfer per unit volume and unit time. The multi-component momentum equation can be expressed as follows:

$$\frac{\partial}{\partial t}\left(\alpha^k \rho^k \mathbf{v}^k\right) + \mathrm{div}\left(\alpha^k \rho^k \mathbf{v}^k \otimes \mathbf{v}^k\right)$$

$$= -\alpha^k \mathrm{grad} p^k - p^k \mathrm{grad}\alpha^k + \mathrm{div}\left(\alpha^k \boldsymbol{\tau}^k\right) - \mathrm{div}\left(\alpha^k \boldsymbol{\tau}^{k''}\right)$$

$$+\alpha^k \sum \boldsymbol{F}^{k,body\ forces} + \boldsymbol{\Omega}'^k \tag{2}$$

where the independent contribution coming from $\alpha^k \rho^k v^k \otimes \mathbf{v}^k$ is the convective flux of momentum, $-\alpha^k \mathrm{grad} p^k - p^k \mathrm{grad}\alpha^k$ is the elastic flux of momentum (pressure tensor), is the viscous, turbulent and diffusive flux of momentum, respectively, $\alpha^k \sum F^{k,body\ forces}$ is the fraction of body forces and $\boldsymbol{\Omega}'^k$ is the internal forces coming from the component interactions. It should be remembered that the interfacial condition for momentum transfer takes a different form to the interfacial mass transfer condition (1) since the momentum transfer $\boldsymbol{\Omega}'^k$ is compensated by surface momentum. The energy equation is defined as follows:

$$\left(\alpha^k \rho^k H^k\right) + \mathrm{div}\left(\alpha^k \rho^k \mathbf{v}^k H^k\right)$$

$$= p^k \frac{\partial \alpha^k}{\partial t} + \alpha^k \frac{\partial p^k}{\partial t} - \mathrm{div}\left(\alpha^k \boldsymbol{q}^k\right) - \mathrm{div}\left(\alpha^k \boldsymbol{q}_H^{k''}\right)$$

$$+\alpha^k \sum \boldsymbol{F}^{k,body\ forces} \cdot \mathbf{v}^k + \Phi_H''^k \tag{3}$$

where H^k is the enthalpy of each component, $\boldsymbol{q}^k$ is the heat flux from each component and $\Phi_H''^k$ is the interfacial energy transfer per unit volume and unit time.

4. The Euler–Euler Spproach to Muliphase Modelling

Further insight into the dynamics of multiphase flows has been provided by the progressive increase of computer power and advances in computational fluid mechanics. There are two ways to perform numerical simulations of multiphase flows: based on either the Euler–Lagrange approach or the Euler–Euler approach [7].

In the Euler–Euler approach the dispersed phase is treated mathematically as a continuum. Conservation equations for each phase are derived to obtain a set of equations which have a similar structure for all phases. The constitutive equations close the equation system by taking into account the structure of the flow field and the material properties by experimental correlations. Eulerian averaging uses spatial, statistical or temporal averages taken in the spatial coordinate system [10]. The Euler–Euler approach introduces the concept of volume fractions, which are assumed to be continuous functions of space and time, and their sum is equal to one, which is shown in Equation (6).

In ANSYS Fluent, three different Euler–Euler multiphase models are available: the volume of fluid model, the mixture model and the Eulerian model [7].

4.1. The Mixture Model

To investigate the effect of phase separation in analysed pipe, the mixture model was used. In general, the mixture model solves the momentum equation for the mixture of any number of phases. The dispersed phase may consist of bubbles, droplets or particulates, and in order to describe that, the model specifies relative velocities. However, the mixture model can also be used without relative velocities for the dispersed phases to model homogeneous multiphase flows. The mixture model has a wide range of applications, including horizontal or vertical flows of gas–liquid mixtures in pipes, bubbly flows, sedimentation and cyclone separators, but it is also applied on particle–fluid mixtures, like fluidized beds. In the mixture model, the volume fraction equation for the secondary phase p can be obtained using Equation (4), which comes from the continuity equation for the secondary phase p.

$$\frac{\partial}{\partial t}(\alpha_p \rho_p) + \nabla(\alpha_p \rho_p \vec{v}_m) = -\nabla\left(\alpha_p \rho_p \vec{v}_{dr,p}\right) + \sum_{q=1}^{n}\left(\dot{m}_{qp} - \dot{m}_{pq}\right) \qquad (4)$$

The volume fraction, denoted by α_p, represents an important parameter in multiphase flow investigations. Volume fractions represent the space occupied by each phase, and the laws of conservation of mass and momentum are satisfied by each phase individually. The volume of the k_{th} phase V_k is defined as:

$$V_k = \int_V \alpha_k \, dV \tag{5}$$

where

$$\sum_{k=1}^{n} \alpha_k = 1 \tag{6}$$

5. Simulation Results

The solutions were obtained using third-order discretization for momentum, volume fraction and turbulence quantities. Different values of carbon dioxide volume fraction were taken into account: 0.05, 0.1, 0.15 and 0.2. These proportions were determined on the basis of thermodynamic analyses of the zero-emission gas cycle with water injection and oxy-firing. The procedure for setting multiphase boundary conditions is slightly different to that for single-phase models. It is necessary to set some conditions separately for individual phases, while other conditions are shared by the mixture. For a velocity inlet, a velocity of 2.5 m/s for each phase was specified; the bubble diameter was equal to 1 mm. Here it is assumed that carbon dioxide at the inlet is moving at the same physical speed as the water.

Table 1. Simulation parameters and results

Case	CO_2 volume fraction	Flow velocity [m/s]	Inlet density [kg/m^3]	Inlet viscosity [kg/m·s]	Outlet 1 density [kg/m^3]	Outlet 1 viscosity [kg/m·s]	Outlet 2 density [kg/m^3]	Outlet 2 viscosity [kg/m·s]
1	0.05	2.5	948.65	0.0009538097	933.46	0.0009387265	971.65	0.0009766387
2	0.1	2.5	898.53	0.000904044	904.12	0.0009095899	970.39	0.0009753935
3	0.15	2.5	848.37	0.0008542428	831.78	0.0008377709	941.07	0.0009462753
4	0.2	2.5	798.31	0.0008045302	769.54	0.0007759667	908.86	0.0009142976

5.1. Velocity Magnitude

Figures 2 through 5 show the velocity magnitude distributions for each case, which are presented as a cross-section of the 3D geometrical model, which capture the most important features of the model in question.

In general, increasing the value of volume fraction leads to a reduction in the velocity magnitude (Figs. 2–5). The mixture stream is split into two parts at the beginning of the upper part of the horizontal arm. The interaction between the flux and the sharp corner leads to the creation of a recirculation pattern, which can be better observed in Figure 6.

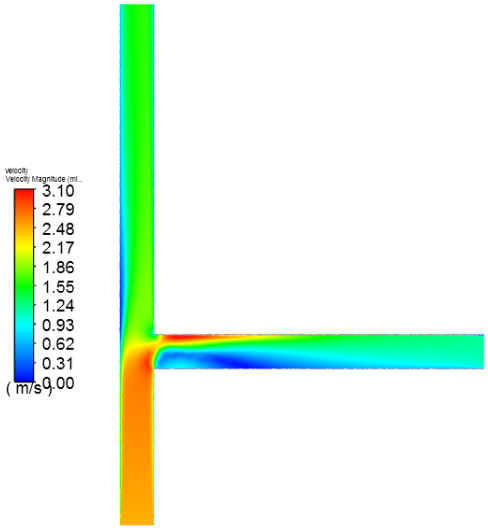

Fig. 2. Contours of velocity magnitude *v* (m/s) – Case 1

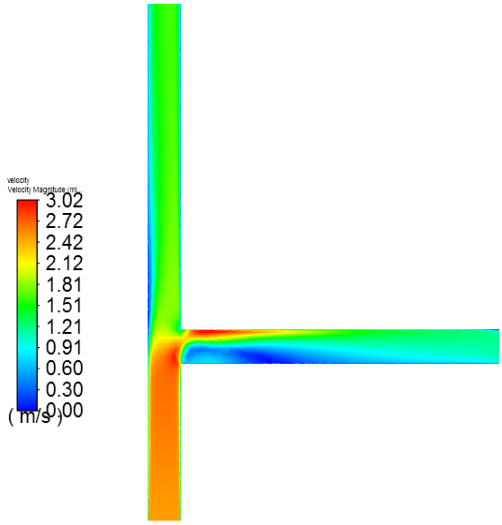

Fig. 3. Contours of velocity magnitude *v* (m/s) – Case 2

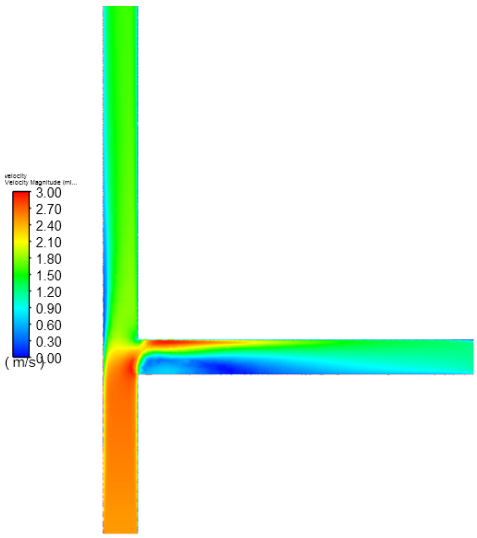

Fig. 4. Contours of velocity magnitude *v* (m/s) – Case 3

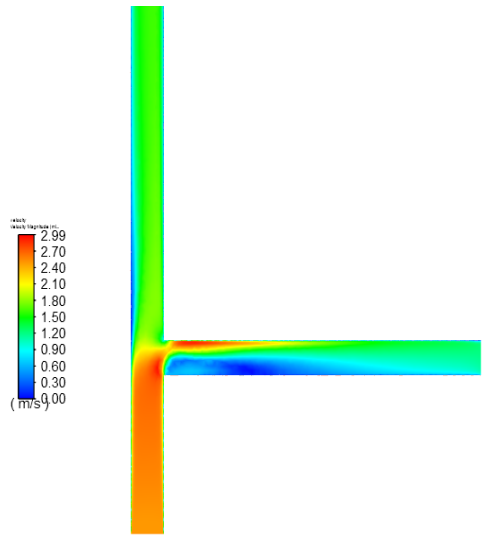

Fig. 5. Contours of velocity magnitude *v* (m/s) – Case 4

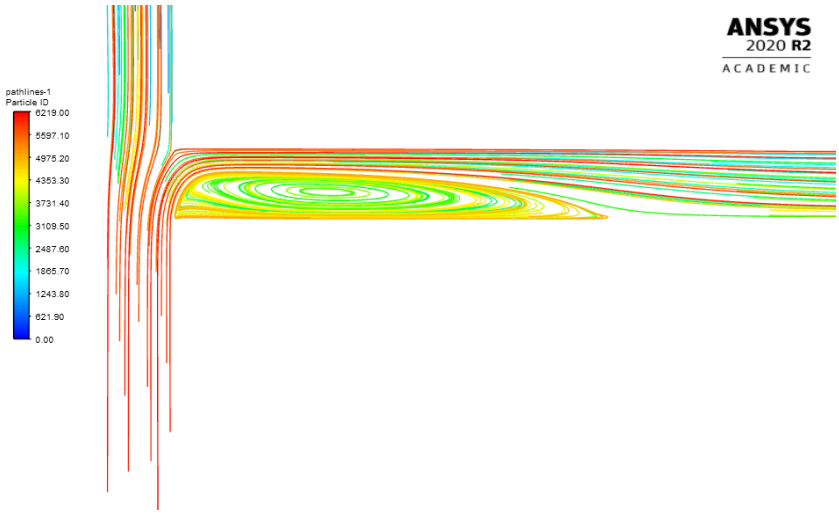

Fig. 6. Contours of particle pathlines, coloured by particle ID

5.2. Pressure Field

Figures 7–14 present the static and dynamic pressure fields for each case.

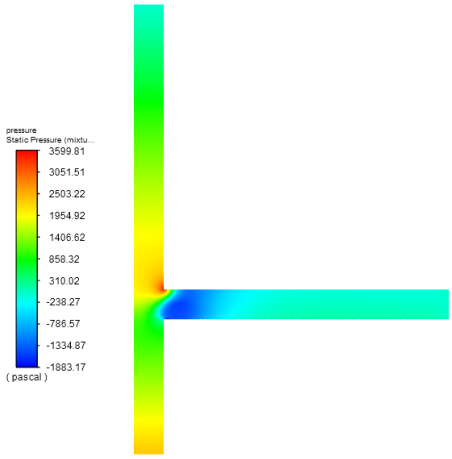

Fig. 7. Contours of static pressure p (Pa) – Case 1

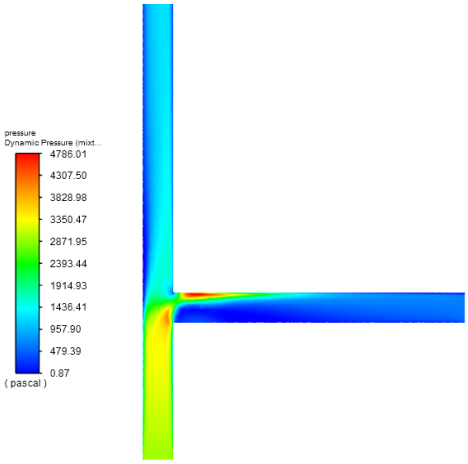

Fig. 8. Contours of dynamic pressure *p* (Pa) – Case 1

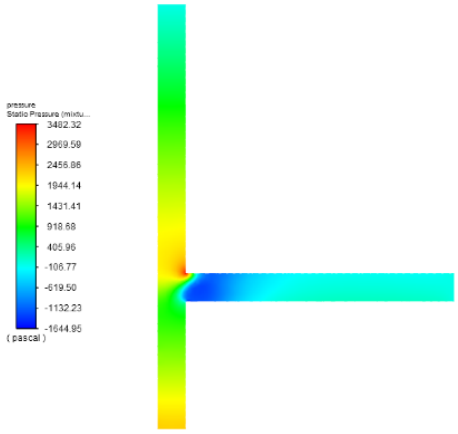

Fig. 9. Contours of static pressure *p* (Pa) – Case 2

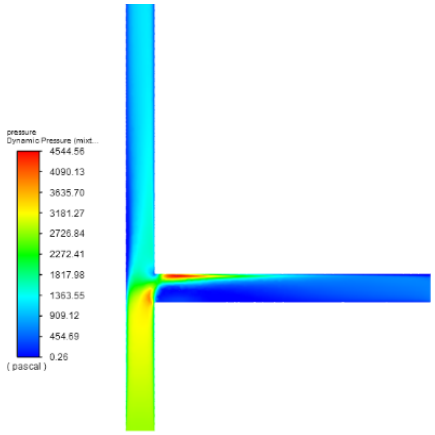

Fig. 10. Contours of dynamic pressure *p* (Pa) – Case 2

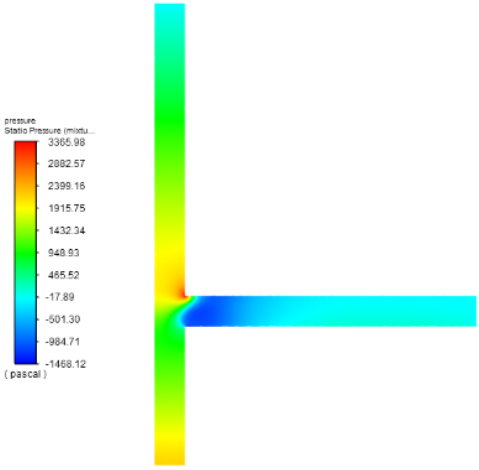

Fig. 11. Contours of static pressure *p* (Pa) – Case 3

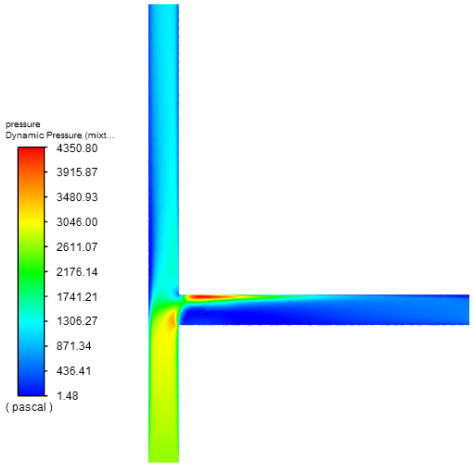

Fig. 12. Contours of dynamic pressure *p* (Pa) – Case 3

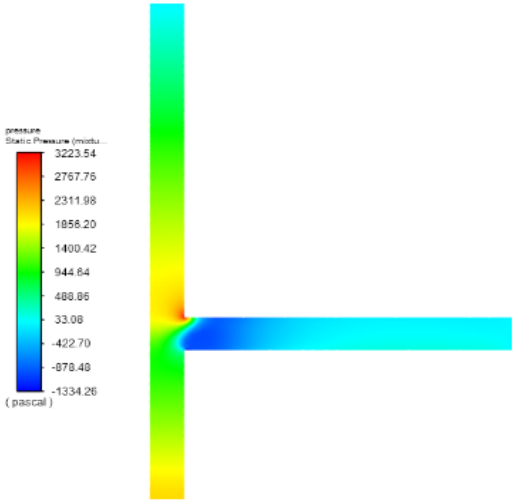

Fig. 13. Contours of static pressure *p* (Pa) – Case 4

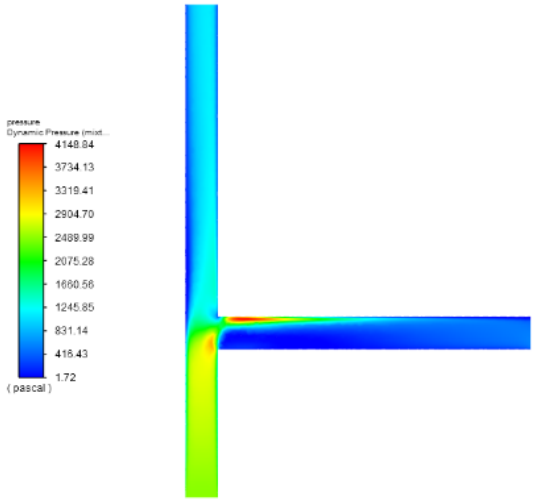

Fig. 14. Contours of dynamic pressure *p* (Pa) – Case 4

Starting from the inlet, it can be observed that after a continuous static pressure drop it suddenly increases near a sharp corner, reaching the maximum value of approximately 3600 Pa for Case 1. To explain that, it seems appropriate to compare this field with the dynamic pressure field. In the area where the higher static pressure begins to disappear, there is an increase in dynamic pressure. This is due to the fluid stream slowing down and the pressure changing from dynamic to static. The dynamic pressure is obtained from the kinetic energy of the particles in motion. In the case of dynamic pressure, its increases and decreases are also influenced by increasing or decreasing friction.

Due to the Operating Density parameter being set to 0, which is necessary when one of the fluid phases is compressible [7], a hydrostatic pressure gradient is observable in the vertical arm. This pressure gradient is reduced while the value of volume fraction increases (Figs. 7, 9, 11 and 13).

5.3. Volume Fraction

Figures 15–18 present contours of carbon-dioxide volume fractions for each case.

When gravity acts downwards, it induces stratification in the side arm of the T-junction. In Figures 15–18, it can be observed that the gas (carbon dioxide) tends to concentrate on the upper part of the side arm. In this case, gravity acts against the inertia that tends to concentrate gas on the lower pressure side and create gas pockets. In the vertical arm, both the gas and the water have velocities in the same direction, and therefore there is no separation. The outflow split greatly modifies the relation between inertia forces and gravity and has an important role in flow distribution and the gas concentration.

As the dispersed phase bubbles travel along the side arm with the flow, this velocity gradient induces a lift force, which tends to oppose the buoyancy force, thereby delaying the accumulation of the carbon dioxide concentration along the top surface of the side arm. In this case, the carbon dioxide volume concentration is relatively small, so the mixture turbulence model is sufficient to capture the important features of the turbulent flow.

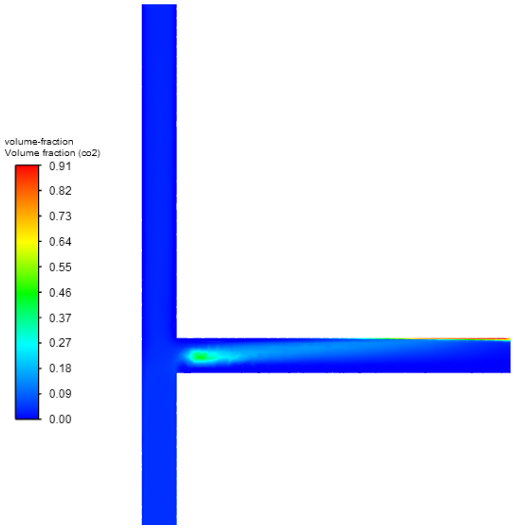

Fig. 15. Contours of CO_2 volume fraction – Case 1

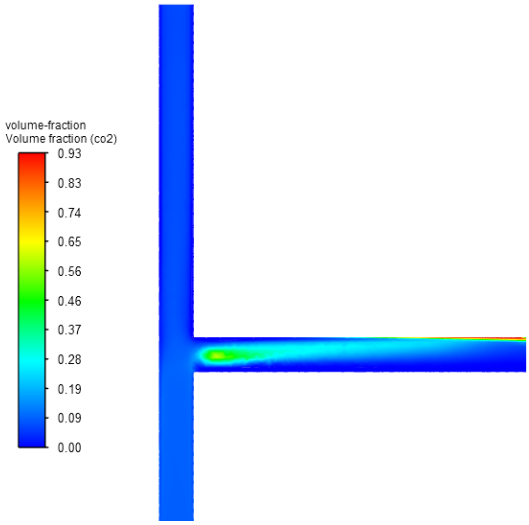

Fig. 16. Contours of CO_2 volume fraction – Case 2

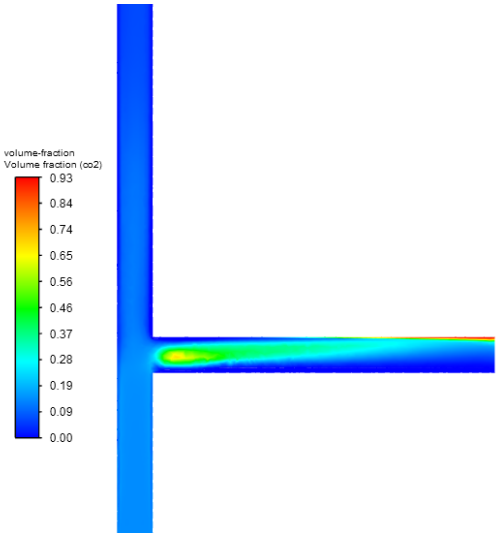

Fig. 17. Contours of CO_2 volume fraction – Case 3

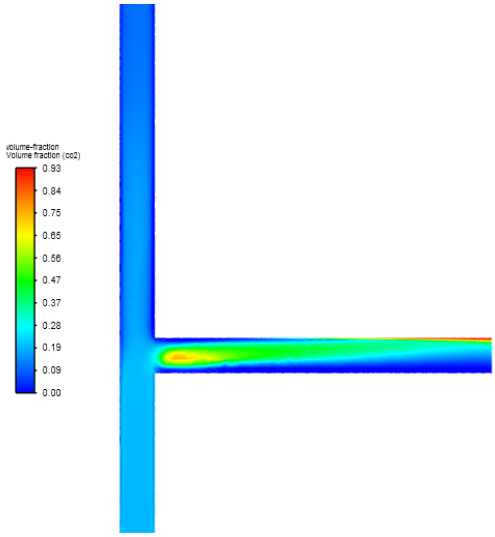

Fig. 18. Contours of CO_2 volume fraction – Case 4

6. Summary

In this article, the multiphase flow of water – a carbon dioxide mixture in a 3D duct – was studied. The solution was obtained using a mixture model. Taking

into account four different volume fraction values of the secondary phase allowed the flow phenomena in T-junctions to be observed and the nature of the water–carbon dioxide multiphase flow to be better understood. When a two-phase flow enters a T-junction, a redistribution of phases often occurs. This redistribution can be desirable for certain situations, where phase separation is required. In some situations, it may lead to reduced efficiency of pipeline systems. Thanks to the model, the volume fractions, pressure fields and velocity fields can be determined, but further experimental verification is necessary in the future. Furthermore, in order to separate gas from liquids more efficiently, it is recommended to introduce an arc to ensure the contribution of centrifugal force in the CO_2 separation process.

Acknowledgements

The article has been prepared within the frame of the project "Negative CO_2 emission gas power plant" – NOR/POLNORCCS/NEGATIVE-CO2-PP/0009/2019. The project is co-financed by POLNOR 2019 under the Norwegian Financial Mechanism 2014–2021.

Literature

[1] Ziółkowski P., Badur J., *A study of a compact high-efficiency zero-emission power plant with oxy-fuel combustion.* In: Stanek W., Gładysz P., Werle S., Adamczyk W., editors. ECOS 2019, Proceedings of the 32nd International Conference on Efficiency, Cost, Optimization, Simulation and Environmental Impact of Energy Systems, Wroclaw, Poland, 23–28 June 2019, published by Institute of Thermal Technology Copyright, Institute of Thermal Technology, Silesian University of Technology 2019: Available: http://www.s-conferences.eu/ecos2019, pp. 1557–1568.

[2] Tryggvason G., Scardovelli R., Zaleski S. *Direct Numerical Simulations of Gas-Liquid Multiphase Flows*, Cambridge University Press, 2011.

[3] Borghi R., Anselmet F., *Turbulent Multiphase Flows with Heat and Mass Transfer*, ISTE Ltd., 2014.

[4] Ferziger J. H., Perić M., *Computational Methods for Fluid Dynamics,* Springer, 3rd Edition, 2002.

[5] Brennen Ch. E., *Fundamentals of Multiphase Flows*, Cambridge University Press, ISBN 0521 848040, 2005.

[6] Crowe C. T., *Multiphase Flow Handbook*, CRC Press, 2006.

[7] ANSYS®, *Academic Research Mechanical and CFD*, Release 19.0, 2019.

[8] Guan Heng Yeoh, Jiyuan Tu, *Computational Techniques for Multi-Phase Flows*, Elsevier Ltd., 351–354, 2010.

[9] Kornet S., Badur J., *Comparison of two models of condensation.* PhD Interdisciplinary Journal, 193–203, 2014.
[10] Manninen M., Taivassalo V., Kaillo S., *On the Mixture Model for Multiphase Flow* VTT Energy Publications 288, 12–21, 1996.